

The top-quark EW couplings in the SMEFT

42nd International Conference on High Energy Physics

Prague, 18th July 2024

Víctor Miralles

in collaboration with:

F. Cornet-Gómez, Marcos Miralles López,

María Moreno Llácer, Marcel Vos

Extension of [2205.02140]

Also based on [1907.10619], [2107.13917] and [2206.08326]



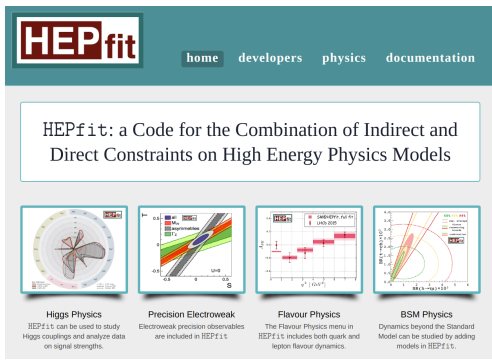
The University of Manchester

Introduction

- Our goal is to constrain all the top-quark related Wilson coefficients of the SMEFT
- The fits have been performed using HEPfit [[1910.14012](#)]
- Estimations on the improvement of the measurements are presented for the HL-LHC
- Estimation for the relevant observables for this fit in future lepton colliders are shown
- Prospects for our limits in the HL-LHC and future lepton colliders are obtained

Fitting tools

- Open source written in C++
- Based on the Bayesian Analysis Toolkit [A. Caldwell, D. Kollar, K. Kröninger, 0808.2552]
- Sampling likelihoods with MCMC
- Supports SM, implemented NP extensions, and the SMEFT



[HEPfit webpage](#) [J. de Blas et al., 1910.14012]

For HEPfit in 2HDMs look at Anirban Karan talk: Status of the Aligned two Higgs doublet model in the low mass region

Other frameworks for SMEFT global fits: [SMEFit, 2105.00006, 2302.06660, 2404.12809], [Fitmaker, 2012.02779], [Aebischer et al., 1810.07698], [Allwicher et al., 2311.00020], [Cirigliano et al., 2311.00021], [Bartocci et al., 2311.04963], [Garosi et al., 2310.00047],...

SMEFT operators relevant for the top-quark

2-quark operators

Couplings of the t- and b-quark to the Z

$$O_{\varphi Q}^3 \equiv (\bar{Q} \tau^I \gamma^\mu Q) (\varphi^\dagger i \overleftrightarrow{D}_\mu^I \varphi)$$

$$O_{\varphi Q}^1 \equiv (\bar{Q} \gamma^\mu Q) (\varphi^\dagger i \overleftrightarrow{D}_\mu \varphi)$$

$$O_{\varphi t(b)} \equiv (\bar{t}(\bar{b}) \gamma^\mu t(b)) (\varphi^\dagger i \overleftrightarrow{D}_\mu \varphi)$$

Chromo-magnetic dipole op.

$$O_{tG} \equiv (\bar{Q} \sigma^{\mu\nu} T^A t) (\varepsilon \varphi^* G_{\mu\nu}^A)$$

EW dipole operators

$$O_{uW} \equiv (\bar{Q} \tau^I \sigma^{\mu\nu} t) (\varepsilon \varphi^* W_{\mu\nu}^I)$$

$$O_{tB} \equiv (\bar{Q} \sigma^{\mu\nu} t) (\varepsilon \varphi^* B_{\mu\nu})$$

t-quark yukawa

$$O_{t\varphi} \equiv (\bar{Q} t) (\varepsilon \varphi^* \varphi^\dagger \varphi)$$

4-quark operators

Couplings of light quarks with t- and b-quarks

$$O_{tu}^{(8)(1)} \quad O_{td}^{(8)(1)} \quad O_{Qq}^{(1,8)(1,1)} \quad O_{Qu}^{(8)(1)} \quad O_{Qd}^{(8)(1)} \quad O_{Qq}^{(3,8)(3,1)} \quad O_{tq}^{(8)(1)}$$

2-quark 2-lepton operators

Couplings of light leptons with t- and b-quarks

$$O_{eb} \quad O_{lb} \quad O_{et} \quad O_{lt} \quad O_{eQ} \quad O_{lQ}^+ \quad O_{lQ}^-$$

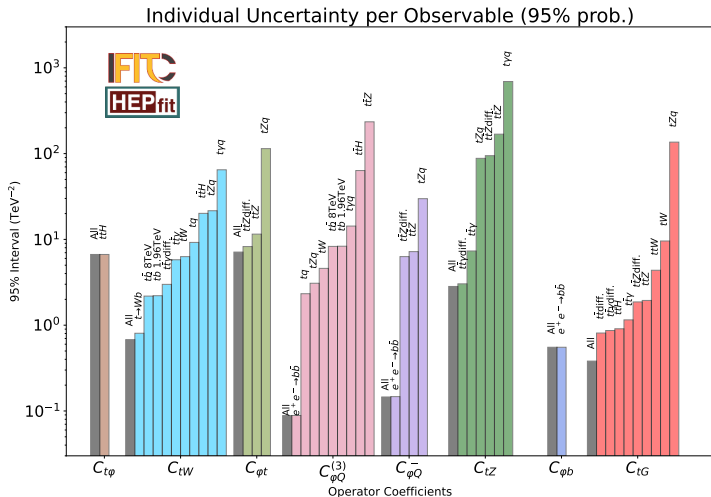
Observables from current colliders (LEP/SLC, Tevatron, LHC run 1 & 2)

- Parametrisations obtained with SMEFT@NLO in MadGraph

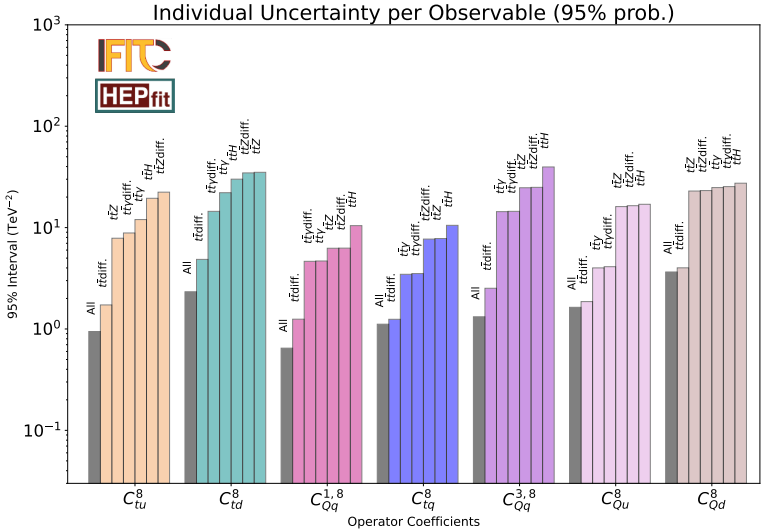
Process	Observable	\sqrt{s}	$\int \mathcal{L}$	Experiment
$pp \rightarrow t\bar{t}$	$d\sigma/dm_{t\bar{t}}$ (15+3 bins)	13 TeV	140 fb^{-1}	CMS
$pp \rightarrow t\bar{t}$	$dA_C/dm_{t\bar{t}}$ (4+2 bins)	13 TeV	140 fb^{-1}	ATLAS
$pp \rightarrow t\bar{t}Z$	$d\sigma/dp_T^Z$ (8 bins)	13 TeV	140 fb^{-1}	ATLAS
$pp \rightarrow t\bar{t}\gamma$	$d\sigma/dp_T^\gamma$ (11 bins)	13 TeV	140 fb^{-1}	ATLAS
$pp \rightarrow t\bar{t}H$	$d\sigma/dp_T^H$ (6 bins)	13 TeV	140 fb^{-1}	ATLAS
$pp \rightarrow tZq$	σ	13 TeV	77.4 fb^{-1}	CMS
$pp \rightarrow t\gamma q$	σ	13 TeV	36 fb^{-1}	CMS
$pp \rightarrow t\bar{t}W$	σ	13 TeV	36 fb^{-1}	CMS
$pp \rightarrow t\bar{b}$ (s-ch)	σ	8 TeV	20 fb^{-1}	LHC
$pp \rightarrow tW$	σ	8 TeV	20 fb^{-1}	LHC
$pp \rightarrow tq$ (t-ch)	σ	8 TeV	20 fb^{-1}	LHC
$t \rightarrow Wb$	F_0, F_L	8 TeV	20 fb^{-1}	LHC
$p\bar{p} \rightarrow t\bar{b}$ (s-ch)	σ	1.96 TeV	9.7 fb^{-1}	Tevatron
$e^-e^+ \rightarrow b\bar{b}$	R_b, A_{FBLR}^{bb}	$\sim 91 \text{ GeV}$	202.1 pb^{-1}	LEP/SLD

Current individual constraints on 2-quark operators

The basis is rotated following the prescription of the LHC top-quark working group: $C_{tZ} = \cos \theta_W C_{tW} - \sin \theta_W C_{tB}$, $C_{\varphi Q}^- = C_{\varphi Q}^{(1)} - C_{\varphi Q}^{(3)}$



Current individual constraints on 4-quark operators



High Luminosity LHC

Prospects for Measurements at HL-LHC

Theoretical Uncertainties \longrightarrow scale with $1/2$

Experimental Uncertainties $\left\{ \begin{array}{l} \text{Modelling} \longrightarrow \text{scale with } 1/2 \\ \text{Systematic} \longrightarrow \text{scale with } 1/\sqrt{\mathcal{L}} \\ \text{Statistical} \longrightarrow \text{scale with } 1/\sqrt{\mathcal{L}} \end{array} \right.$

Prospects for Measurements at HL-LHC

Inclusive cross sections and helicities

Process	Measured (fb)	SM (fb)	LHC Unc.					HL-LHC Unc.				
			theo.	exp.				theo.	exp.			
				stat.	sys.	mod.	tot.		stat.	sys.	mod.	tot.
$pp \rightarrow t\bar{t}H + tHq$	640	664.3	41.7	90	40	70.7	121.2	20.9	19.4	8.6	35.4	41.3
$pp \rightarrow t\bar{t}Z$	990	810.9	85.8	51.5	48.9	67.3	97.8	42.9	11.1	10.6	33.6	37.0
$pp \rightarrow t\bar{t}\gamma$	39.6	38.5	1.76	0.8	1.25	2.16	2.62	0.88	0.17	0.27	1.08	1.13
$pp \rightarrow tZq$	111	102	3.5	13.0	6.1	6.2	15.7	1.75	2.09	0.98	3.1	3.87
$pp \rightarrow t\gamma q$	115.7	81	4	17.1	21.1	21.1	34.4	2	1.9	2.3	10.6	11.0
$pp \rightarrow t\bar{t}W + EW$	770	647.5	76.1	120	59.6	73.0	152.6	38.1	13.1	6.5	36.5	39.4
$pp \rightarrow t\bar{b} (s\text{-ch})$	4900	5610	220	784	936	790	1454	110	35	42	395	399
$pp \rightarrow tW$	23100	22370	1570	1086	2000	2773	3587	785	49	89	1386	1390
$pp \rightarrow tq (t\text{-ch})$	87700	84200	250	1140	3128	4766	5810	125	51	140	2383	2390
F_0	0.693	0.687	0.005	0.009	0.006	0.009	0.014	0.003	0.0004	0.0003	0.004	0.004
F_L	0.315	0.311	0.005	0.006	0.003	0.008	0.011	0.003	0.0003	0.0002	0.004	0.004

Prospects for Measurements at HL-LHC

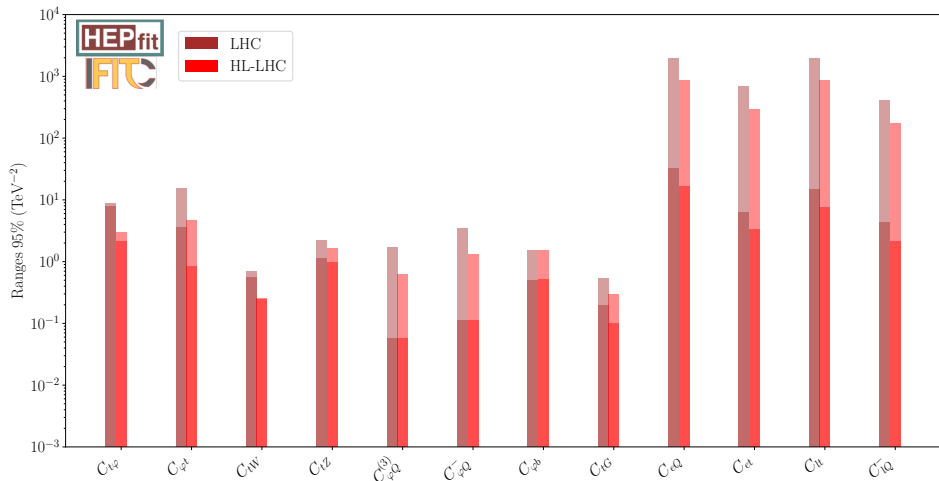
ATLAS is making efforts to measure $pp \rightarrow t\bar{t}\ell\ell$

From MsC Thesis of Abel Gutiérrez Camacho:

Process	Inclusive (10^{-6} pb)	Differential: $m_{\ell\bar{\ell}}$ (GeV)			
		100-120	120-140	140-180	> 180
$pp \rightarrow t\bar{t}\ell\ell$	1830	1000	340	230	260
Unc. LHC	915	490	235	200	260
Unc. HL-LHC	400	190	85	70	99

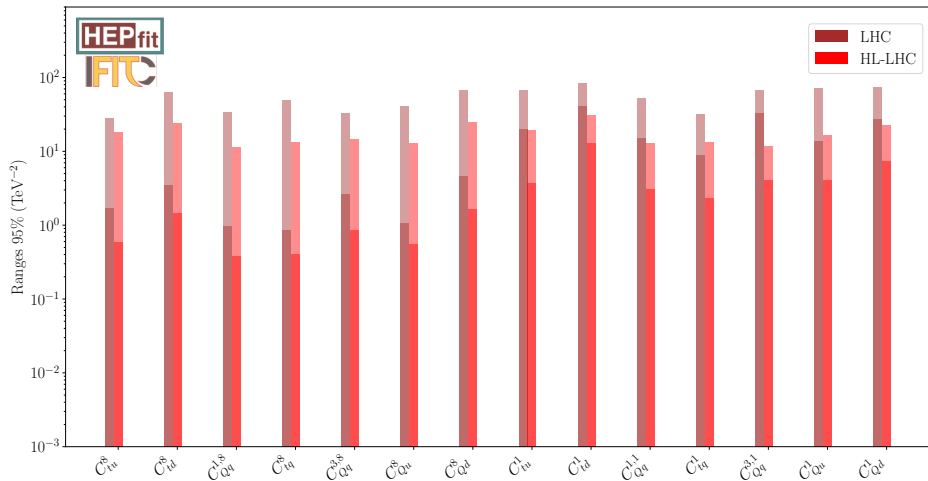
Current constraints vs expected HL-LHC constraints

Shadowed (solid) bars → marginalised from global (individual) fit



Current constraints vs expected HL-LHC constraints

Shadowed (solid) bars → marginalised from global (individual) fit



Future lepton colliders

Measurements at e^+e^- colliders: $b\bar{b}$ production

Machine	Polarisation	Energy	Luminosity	Observable
ILC	$P(e^+, e^-):(-30\%, +80\%)$ $P(e^+, e^-):(+30\%, -80\%)$	250 GeV	2 ab^{-1}	$\sigma_{b\bar{b}}$ $A_{\text{FB}}^{b\bar{b}}$
		500 GeV	4 ab^{-1}	
		1 TeV	8 ab^{-1}	
CLIC	$P(e^+, e^-):(0\%, +80\%)$ $P(e^+, e^-):(0\%, -80\%)$	380 GeV	2 ab^{-1}	$\sigma_{b\bar{b}}$ $A_{\text{FB}}^{b\bar{b}}$
		1.5 TeV	2.5 ab^{-1}	
		3 TeV	5 ab^{-1}	
CEPC/FCC-ee	Unpolarised	Z-pole	$57.5/150 \text{ ab}^{-1}$	$\sigma_{b\bar{b}}$ $A_{\text{FB}}^{b\bar{b}}$
		240 GeV	$20/5 \text{ ab}^{-1}$	
		360/365 GeV	$1/1.5 \text{ ab}^{-1}$	

- Expected uncertainties from [\[A. Irles, et al., 2403.09144\]](#)
- These observables set constraints on the EW precision observables $C_{\varphi Q}^+ = C_{\varphi Q}^1 + C_{\varphi Q}^3$ and $C_{\varphi b}$
- Also relevant for 2-quark 2-lepton operators C_{lQ}^+ , C_{lb} and C_{eb}
- The higher-energy measurement are more relevant for the 2-quark 2-lepton operators

Measurements at e^+e^- colliders: $t\bar{t}$ production

Machine	Polarisation	Energy	Luminosity	Observable
ILC	$P(e^+, e^-):(-30\%, +80\%)$	500 GeV	4 ab^{-1}	Optimal
	$P(e^+, e^-):(+30\%, -80\%)$	1 TeV	8 ab^{-1}	Observables
CLIC	$P(e^+, e^-):(0\%, +80\%)$ $P(e^+, e^-):(0\%, -80\%)$	380 GeV	2 ab^{-1}	Optimal Observables
		1.5 TeV	2.5 ab^{-1}	
		3 TeV	5 ab^{-1}	
CEPC/FCC- ee	Unpolarised	350 GeV	0.2 ab^{-1}	Optimal Observables
		365 GeV	$1/1.5 \text{ ab}^{-1}$	

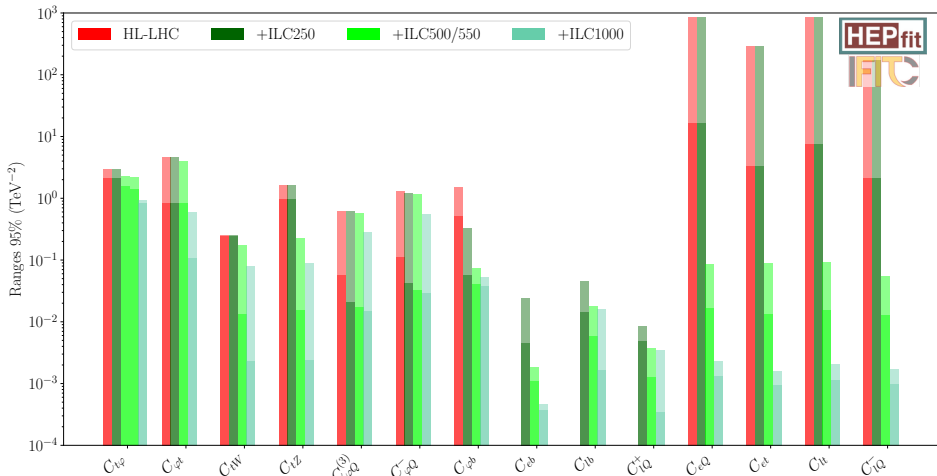
- Optimal observables maximally exploit the information in the fully differential $e^+e^- \rightarrow t\bar{t} \rightarrow bW^+\bar{b}W^-$ distribution [1807.02121]
- These constrain the 2-fermion operators $C_{\varphi Q}^-$, $C_{\varphi t}$, C_{tW} and C_{tZ}
- Also the 2-quark 2-lepton operators C_{lQ}^- , C_{lt} , C_{et} and C_{eQ}
- With these we eliminate blind directions in the $C_{\varphi Q}^{(1)} - C_{\varphi Q}^{(3)}$ plane
- Two different energies above the $t\bar{t}$ threshold are need to constrain all the 2- and 4-fermion operators

Measurements at e^+e^- colliders: $t\bar{t}H$ production

Machine	Polarisation	Energy	Luminosity	Observable
ILC	$P(e^+, e^-):(-30\%, +80\%)$	500/550 GeV	4 ab^{-1}	Inclusive cross section
	$P(e^+, e^-):(+30\%, -80\%)$	1 TeV	8 ab^{-1}	
CLIC	$P(e^+, e^-):(0\%, +80\%)$ $P(e^+, e^-):(0\%, -80\%)$	1.5 TeV	2.5 ab^{-1}	Inclusive cross section

- Essential measurement in order to improve the limits on the top-quark Yukawa
- The effect of a ILC run at 550 GeV has been studied
- At ILC550 the production cross section increases a factor of 3 w.r.t. ILC500 improving the statistical sensitivity by more than a 50%
- ILC550 and CLIC1500 have a similar sensitivity as HL-LHC
- ILC1000 improves the expected HL-LHC sensitivity by a factor of two

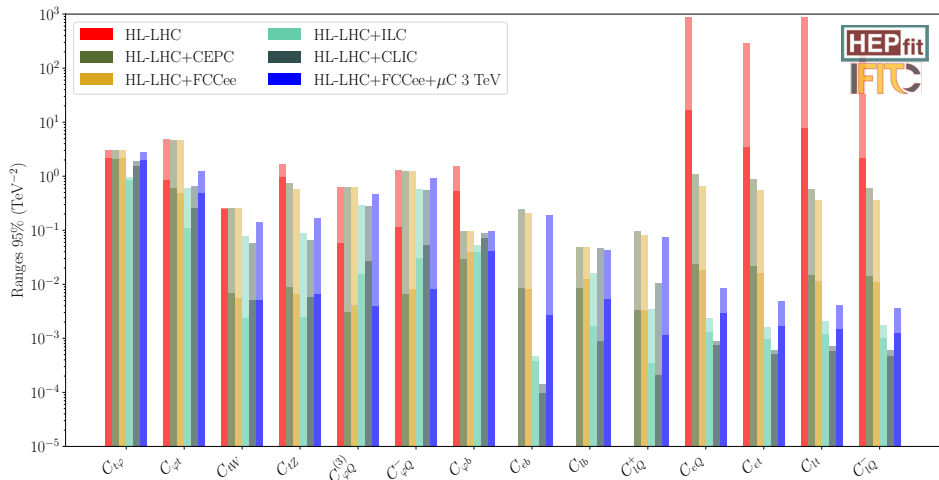
Expected constraints for different e^+e^- operation energies



Measurements at a muon colliders

Machine	Polarisation	Energy	Luminosity	Observable
Muon Collider	Unpolarised	3 TeV	1 ab ⁻¹	$\sigma_{b\bar{b}}, A_{\text{FB}}^{b\bar{b}}$
		10 TeV	10 ab ⁻¹	Optimal Observables ($t\bar{t}$ s-channel)
		30 TeV	90 ab ⁻¹	$t\bar{t}$ VBF $t\bar{t}H$

Comparison of future colliders



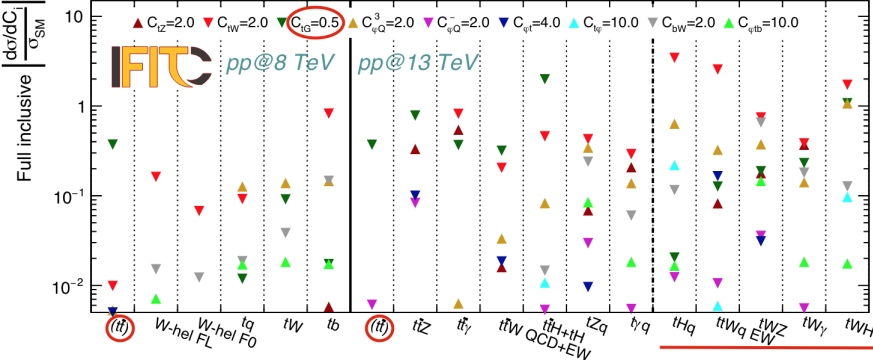
Summary

- HL-LHC expected to improve the bounds by roughly a factor 3
- Lepton colliders can significantly improve bounds on bottom- and on top-quark operators, if operated above the $t\bar{t}$ threshold
- Circular colliders operated at and slightly above the $t\bar{t}$ threshold can improve bottom- and top- operators by factor 5 and 2 for 2-fermion operators.
- Power to constrain 4-fermion operators limited by energy reach
- Linear colliders can provide very tight bounds on all operators
- Significant improvements for the limits on the top-quark yukawa are found when operating above 550 GeV

Thank you!

Back up

Sensitivity

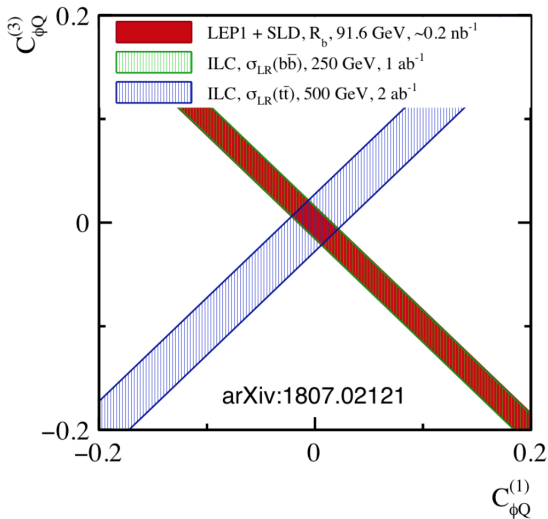


Future Colliders - Complementarity on e^+e^- Colliders

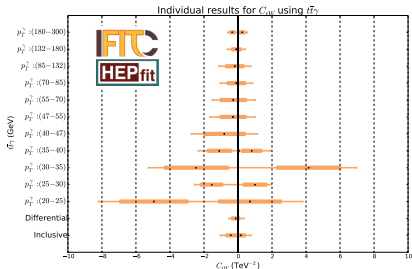
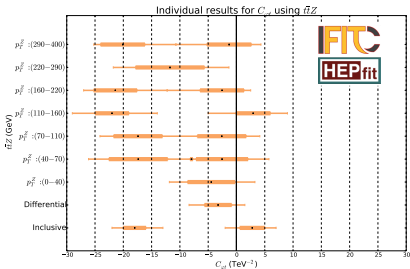
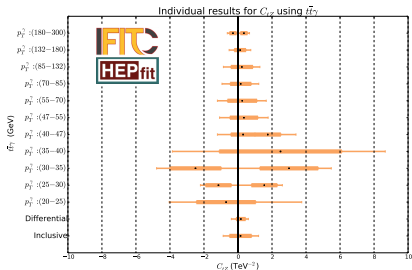
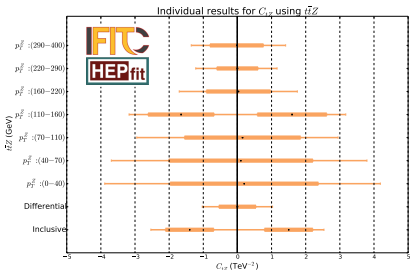
Good complementarity between $b\bar{b}$ (LEP) and $t\bar{t}$ (future e^+e^- collider) if we reach $\sqrt{s} > 2m_t$

$$\delta g_L^t = -(C_{\phi Q}^1 - C_{\phi Q}^3)m_t^2/\Lambda^2$$

$$\delta g_L^b = -(C_{\phi Q}^1 + C_{\phi Q}^3)m_t^2/\Lambda^2$$

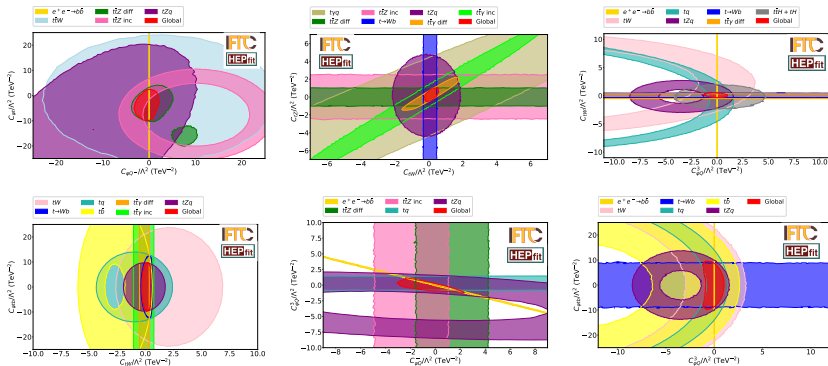


Results - Differential Cross Section Effect



Results - Complementarity Between Observables

- Very good complementarity between the observables
- The data set is diverse enough to avoid the existence of blind directions



Dependencies

[1910.03606]

parameter	$t\bar{t}$	single t	tW	tZ	t decay	$t\bar{t}Z$	$t\bar{t}W$
$C_{Qq}^{1,8}$	Λ^{-2}	–	–	–	–	Λ^{-2}	Λ^{-2}
$C_{Qq}^{3,8}$	Λ^{-2}	$\Lambda^{-4} [\Lambda^{-2}]$	–	$\Lambda^{-4} [\Lambda^{-2}]$	$\Lambda^{-4} [\Lambda^{-2}]$	Λ^{-2}	Λ^{-2}
C_{tu}^8, C_{td}^8	Λ^{-2}	–	–	–	–	Λ^{-2}	–
$C_{Qq}^{1,1}$	$\Lambda^{-4} [\Lambda^{-2}]$	–	–	–	–	$\Lambda^{-4} [\Lambda^{-2}]$	$\Lambda^{-4} [\Lambda^{-2}]$
$C_{Qq}^{3,1}$	$\Lambda^{-4} [\Lambda^{-2}]$	Λ^{-2}	–	Λ^{-2}	Λ^{-2}	$\Lambda^{-4} [\Lambda^{-2}]$	$\Lambda^{-4} [\Lambda^{-2}]$
C_{tu}^1, C_{td}^1	$\Lambda^{-4} [\Lambda^{-2}]$	–	–	–	–	$\Lambda^{-4} [\Lambda^{-2}]$	–
C_{Qu}^8, C_{Qd}^8	Λ^{-2}	–	–	–	–	Λ^{-2}	–
C_{tq}^8	Λ^{-2}	–	–	–	–	Λ^{-2}	Λ^{-2}
C_{Qu}^1, C_{Qd}^1	$\Lambda^{-4} [\Lambda^{-2}]$	–	–	–	–	$\Lambda^{-4} [\Lambda^{-2}]$	–
C_{tq}^1	$\Lambda^{-4} [\Lambda^{-2}]$	–	–	–	–	$\Lambda^{-4} [\Lambda^{-2}]$	$\Lambda^{-4} [\Lambda^{-2}]$
$C_{\phi Q}^-$	–	–	–	Λ^{-2}	–	Λ^{-2}	–
$C_{\phi Q}^3$	–	Λ^{-2}	Λ^{-2}	Λ^{-2}	Λ^{-2}	–	–
$C_{\phi t}$	–	–	–	Λ^{-2}	–	Λ^{-2}	–
$C_{\phi tb}$	–	Λ^{-4}	Λ^{-4}	Λ^{-4}	Λ^{-4}	–	–
C_{tZ}	–	–	–	Λ^{-2}	–	Λ^{-2}	–
C_{tW}	–	Λ^{-2}	Λ^{-2}	Λ^{-2}	Λ^{-2}	–	–
C_{bW}	–	Λ^{-4}	Λ^{-4}	Λ^{-4}	Λ^{-4}	–	–
C_{tG}	Λ^{-2}	$[\Lambda^{-2}]$	Λ^{-2}	–	$[\Lambda^{-2}]$	Λ^{-2}	Λ^{-2}

Table 1. Wilson coefficients in our analysis and their contributions to top-quark observables via SM-interference (Λ^{-2}) and via dimension-6 squared terms only (Λ^{-4}). A square bracket indicates that the Wilson coefficient contributes via SM-interference at NLO QCD. All quark masses except m_t are assumed to be zero. ‘Single t ’ stands for s - and t -channel electroweak top production.

Theoretical Framework

- We use an EFT description to parametrise deviations from the SM

Relevant Operators			
Coefficient	Operator	Coefficient	Operator
$C_{\varphi Q}^1$	$(\bar{Q}\gamma^\mu Q) (\varphi^\dagger i \overleftrightarrow{D}_\mu \varphi)$	$C_{\varphi Q}^3$	$(\bar{Q}\tau^I \gamma^\mu Q) (\varphi^\dagger i \overleftrightarrow{D}_\mu^I \varphi)$
$C_{\varphi t}$	$(\bar{t}\gamma^\mu t) (\varphi^\dagger i \overleftrightarrow{D}_\mu \varphi)$	$C_{\varphi b}$	$(\bar{b}\gamma^\mu b) (\varphi^\dagger i \overleftrightarrow{D}_\mu \varphi)$
$C_{t\varphi}$	$(\bar{Q}t) (\varepsilon\varphi^* \varphi^\dagger \varphi)$	C_{tG}	$(\bar{t}\sigma^{\mu\nu} T^A t) (\varepsilon\varphi^* G_{\mu\nu}^A)$
C_{tW}	$(\bar{Q}\tau^I \sigma^{\mu\nu} t) (\varepsilon\varphi^* W_{\mu\nu}^I)$	C_{tB}	$(\bar{Q}\sigma^{\mu\nu} t) (\varepsilon\varphi^* B_{\mu\nu})$
$C_{qq}^{1(ijkl)}$	$(\bar{q}_i \gamma^\mu q_j) (\bar{q}_k \gamma_\mu q_l)$	$C_{qq}^{3(ijkl)}$	$(\bar{q}_i \tau^I \gamma^\mu q_j) (\bar{q}_k \tau^I \gamma_\mu q_l)$
$C_{uu}^{(ijkl)}$	$(\bar{u}_i \gamma^\mu u_j) (\bar{u}_k \gamma_\mu u_l)$	$C_{ud}^{8(ijkl)}$	$(\bar{u}_i \gamma^\mu T^A u_j) (\bar{d}_k \gamma_\mu T^A d_l)$
$C_{qu}^{8(ijkl)}$	$(\bar{q}_i \gamma^\mu T^A q_j) (\bar{u}_k \gamma_\mu T^A u_l)$	$C_{qd}^{8(ijkl)}$	$(\bar{q}_i \gamma^\mu T^A q_j) (\bar{d}_k \gamma_\mu T^A d_l)$
C_{lQ}^1	$(\bar{Q}\gamma_\mu Q) (\bar{l}\gamma^\mu l)$	C_{lQ}^3	$(\bar{Q}\tau^I \gamma_\mu Q) (\bar{l}\tau^I \gamma^\mu l)$
C_{lt}	$(\bar{t}\gamma_\mu t) (\bar{l}\gamma^\mu l)$	C_{lb}	$(\bar{b}\gamma_\mu b) (\bar{l}\gamma^\mu l)$
C_{eQ}	$(\bar{Q}\gamma_\mu Q) (\bar{e}\gamma^\mu e)$	C_{et}	$(\bar{t}\gamma_\mu t) (\bar{e}\gamma^\mu e)$
C_{eb}	$(\bar{b}\gamma_\mu b) (\bar{e}\gamma^\mu e)$	–	–

Theoretical Framework

- The Wilson coefficients are fitted are:

Coefficients Fitted			
2-quark	C_{tG} $C_{\phi t}$ -	$C_{\phi Q}^3$ $C_{\phi b}$ $C_{t\phi}$	$C_{\phi Q}^- = C_{\phi Q}^1 - C_{\phi Q}^3$ $C_{tZ} = c_W C_{tW} - s_W C_{tB}$ C_{tW}
4-quark	$C_{tu}^8 = \sum_{i=1,2} 2C_{uu}^{(i33i)}$ $C_{Qu}^8 = \sum_{i=1,2} C_{qu}^{(33ii)}$ -	$C_{td}^8 = \sum_{i=1,2,3} C_{ud}^{(8(33ii))}$ $C_{Qd}^8 = \sum_{i=1,2,3} C_{qd}^{(8(33ii))}$ -	$C_{Qq}^{1,8} = \sum_{i=1,2} C_{qq}^{1(i33i)} + 3C_{qq}^{3(i33i)}$ $C_{Qq}^{3,8} = \sum_{i=1,2} C_{qq}^{1(i33i)} - C_{qq}^{3(i33i)}$ $C_{tq}^8 = \sum_{i=1,2} C_{uq}^{(8(ii33))}$
2-quark 2-lepton	C_{eb} C_{lb} -	C_{et} C_{lt} -	$C_{lQ}^+ = C_{lQ}^1 + C_{lQ}^3$ $C_{lQ}^- = C_{lQ}^1 - C_{lQ}^3$ C_{eQ}

$t\bar{t}H$ at lepton colliders

[1104.5132]

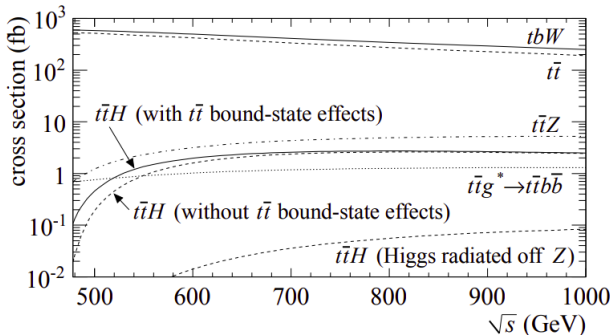


FIG. 2. Production cross section of the $e^+e^- \rightarrow t\bar{t}H$ signal (shown with and without $t\bar{t}$ bound-state effects), together with those of the main background processes, $t\bar{t}H$ (Higgs radiated off the Z boson), $t\bar{t}Z$, $t\bar{t}$, $t\bar{t}W^-/\bar{t}tW^+$ (denoted as $t\bar{t}W$), and $t\bar{t}g^* \rightarrow t\bar{t}b\bar{b}$, as a function of the CM energy without beam polarizations. The initial state radiation and beamstrahlung effects are included.

Comparison of future colliders

